

Role of C–H Bond Strength in the Rate and Selectivity of Oxidative Dehydrogenation of Alkanes

Michael Zboray, Alexis T. Bell,* and Enrique Iglesia*

Chemical Sciences Division, E. O. Lawrence Berkeley National Laboratory and Department of Chemical Engineering, University of California, Berkeley, California 94720-1462

Received: February 20, 2009; Revised Manuscript Received: April 30, 2009

The oxidative dehydrogenation of alkanes (C_2H_6 , C_3H_8 , $i-C_4H_{10}$, and $n-C_4H_{10}$) was investigated on VO_x supported on Al_2O_3 . Rate constants for alkane dehydrogenation (k_1), alkane combustion (k_2), and alkene combustion (k_3) were measured, and a model was developed to describe the effects of alkane composition on these rate constants. The proposed model accounts for the effects of the number of C–H bonds available for activation and the relative strengths of these bonds in both the reactant and the product molecules. The Brønsted–Evans–Polanyi (BEP) relationship is used to relate activation energies of secondary and tertiary C–H bonds to that of primary C–H bonds. The model gives a reasonable approximation of the relative order of alkane reactivity, expressed by $k_1 + k_2$, and the relative ranking of alkanes with respect to combustion versus oxidative dehydrogenation, expressed by k_2/k_1 . The ratio of k_2/k_1 is described by the product of two components: one that depends on the nature, number, and relative strength of C–H bonds of surface alkoxides, and a second one that is independent of the alkoxide composition and structure but depends on the difference in the entropy of activation for CO_x precursor versus alkene formation. The model also explains the observed variation of k_3 with alkene composition by considering two precursor states for alkenes. One is strongly bound through π -orbital interactions with Lewis acid centers, and the second weakly binds via H bonding and van der Waals interactions, similar to the binding of alkanes. As a result, the rate of alkene combustion depends strongly on the large heats of adsorption of alkenes and only slightly on the presence of weak allylic C–H bonds. The high rate of C_2H_4 combustion is thus a consequence of its high heat of adsorption.

Introduction

Oxidative dehydrogenation (ODH) provides an alternate route for the conversion of alkanes to alkenes. It avoids the energy inefficiencies and ubiquitous deactivation of nonoxidative processes. Alkene yields are typically below 50%, even for C_2H_6 , the alkane that leads to the most selective ODH reactions.¹ Yield limitations reflect the sequential nature of the pathways involved and the higher reactivity of allylic C–H bonds, ubiquitous in alkenes, compared with C–H bonds in alkane reactants. Investigations carried out with VO_x -based catalysts have shown that alkane ODH reaction rates are proportional to alkane pressure but independent of O_2 pressure,² consistent with C–H bond activation as the sole kinetically relevant step. Detailed kinetic and isotopic methods have confirmed these conclusions for VO_x and MoO_x catalysts.^{3–8}

Hodnett et al.^{9,10} proposed empirical relations between selectivity and the strength of C–H bonds in reactant and products for reactions involving the activation of these bonds. These relations predict that achievable selectivities at a given reactant conversion depend on the differences in dissociation energies between the weakest C–H bonds in reactants and in products for a broad range of catalytic oxidation reactions.⁹ This approach does not include, however, any effects of the expected differences in the adsorption of reactants and products or any contributions to reactivity from C–H bonds other than the weakest one in each molecule. Low heats of adsorption ($-\Delta H_{ads}$) for alkanes reflect predominant interactions via hydrogen-bonding or van der Waals forces. Alkenes interact with surfaces

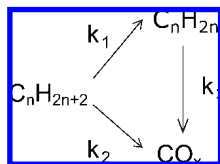
via similar interactions but also bind more strongly onto Lewis acid sites via their electron-rich π orbitals. The stronger binding of alkenes can lead to reactivities much greater than those predicted from their weakest C–H bond, consistent with the modest yields ($\sim 20\%$)¹ often observed for C_2H_4 in spite of its strong C–H bonds (464 kJ mol^{-1} ; ref 11) relative to those in C_2H_6 reactants (421 kJ mol^{-1} ; ref 11). Differences in C–H bond strength between the strongest and the weakest C–H bonds in alkanes are generally less than 20 kJ mol^{-1} , and ubiquitous linear free energy relations^{12,13} suggest their differences in activation barriers are even smaller. As a result, stronger bonds increasingly contribute to measured rates as temperatures increase and must be considered in all relations between catalytic reactivity and C–H bond energies.

The effects of C–H bond dissociation energy on activation energies are typically described by Brønsted–Evans–Polanyi (BEP) relations;^{12,13} these relations express activation energies as a linear function of enthalpy changes for a given elementary step. This approach has proven useful, in spite of its empirical basis, for homogeneous and catalytic reactions, such as in acid catalysis,¹² reactions of benzene derivatives,¹⁴ formate and methoxide decomposition on metals,¹⁵ CO , N_2 , O_2 , and NO activation on metal surfaces,¹⁶ and C–H bond formation and dissociation on metals.¹⁷ For reactions limited by homolytic bond cleavage steps, ΔH_R will depend sensitively on C–H bond dissociation energies, thus allowing C–H bond activation barriers to be related to the strength of individual C–H bonds.

Here, we address apparent inconsistencies between measured activation energies and weakest C–H bond energies and also the low C_2H_4 yields and preferential activation of the weakest

* To whom correspondence should be addressed. E-mail: bell@chem.berkeley.edu; iglesias@berkeley.edu.

SCHEME 1: Pathways in the Oxidative Dehydrogenation of Alkanes



C–H bonds in hydrocarbons by measuring rate constants and activation energies for C_2H_6 , C_3H_8 , $n-C_4H_{10}$, and $i-C_4H_{10}$ using the reaction pathways depicted in Scheme 1. These alkanes were selected because they and their alkene products differ significantly in the number and strength of their C–H bonds. These data were obtained under strict kinetic control by the deconvolution of primary and secondary pathways. Under these conditions, C–H bond activation is the sole kinetically relevant step in the activation of alkanes and alkenes.^{3,6} We find that interpretation of the observed reactivity of alkanes and the distribution of products formed during ODH requires careful consideration of the nature, number, and relative strength of all C–H bonds present in reactant alkanes and product alkenes, as well as the modes by which alkenes can adsorb on the catalyst.

Experimental Methods

Catalyst Synthesis. Vanadia domains supported on alumina were prepared via incipient-wetness impregnation of fumed $\gamma-Al_2O_3$ (Degussa AG, $119\text{ m}^2\text{ g}^{-1}$) with a solution of vanadium(V) oxy-tri-isopropoxide (Sigma-Aldrich, 99%) in 2-propanol (Sigma-Aldrich, 99.9%). This sample contained $\sim 3\%$ wt V_2O_5 . Preparation details have been described previously^{18,19} and are included in the Supporting Information.

Catalyst Characterization. Samples were characterized by N_2 physisorption and Raman and UV–vis spectroscopies using methods reported in the Supporting Information. Surface areas (per mass of support) measured by N_2 physisorption were unchanged by impregnation and thermal treatment. Raman spectra indicate that VO_x species are predominantly present as monovanadates, with traces of V–oxo oligomers but no detectable crystalline V_2O_5 . These conclusions were confirmed by measurements of edge energies in UV–vis spectra, which are consistent with the predominant presence of monovanadate species. The adsorption edge energy was 2.49 eV, and adsorption edge energies above 2.5 eV have been attributed to V^{5+} in tetrahedral coordination environments.²⁰

Catalytic Rates and Selectivity Measurement. Steady-state conversions and selectivities were measured using a quartz packed-bed reactor (11 mm i.d., 13 mm o.d.) equipped with a temperature controller (Watlow) connected to a K-type thermocouple (Omega) in contact with its outer wall. Inlet reactant flow rates were metered by mass flow controllers (Porter Instrument Co.). Catalyst samples (0.1–0.4 g, 250–500 μm) were treated in 10% O_2/He (Praxair, 99.993%, $0.83\text{ cm}^3\text{ s}^{-1}$) at 723 K for 1 h before bringing samples to the desired reaction temperature. The alkane reactants and the respective temperatures used for each were as follows: C_2H_6 (Praxair, 99.9%), 673–748 K; C_3H_8 (Praxair, 99.5%), 598–673 K; $n-C_4H_{10}$ (Praxair, 99.5%), 573–648 K; and $i-C_4H_{10}$ (Praxair, 99.99%), 588–648 K. The alkane and O_2 partial pressures were 8 and 6 kPa, respectively. The catalyst bed was diluted with acid-washed quartz powder (250–500 μm) to maintain plug-flow hydrodynamics and to avoid temperature gradients. Rates were unaffected by quartz/

catalyst mass ratios between 1 and 4. Space velocities were varied between 0.1 to $1.0\text{ cm}^3\text{ (g-cat s)}^{-1}$ at constant inlet reactant pressures. Conversion data were corrected at all conversions greater than 5% using plug-flow formalisms and previously measured alkane ODH rate equations.^{3,6} Reactant and product concentrations were measured by gas chromatography (Agilent 6890) using a capillary column (HP-1, 50 m, 32 μm , 1.05 μm) connected to a flame ionization detector and a packed column (Hayesep-DB, 100/120, 30 ft \times 1/8 in.) connected to a thermal conductivity detector.

Analysis of Reaction Data. Reaction rates and selectivities were measured as a function of reactor residence time, and these data were used to estimate the rate constants shown in Scheme 1. The rates of reactions 1–3 were assumed to be proportional to the pressure of the respective hydrocarbons and independent of O_2 pressure.^{2,3,6} Values for k_1 and k_2 were obtained by extrapolating measured rates to zero residence time. At low alkane conversions ($k_3\tau/3 < 1$), alkene selectivities are given by²¹

$$S_{\text{alkene}} = \frac{k_1}{k_1 + k_2} \left(1 - \frac{k_3}{2} \tau \right) \quad (1)$$

The accuracy of this approximate expression was checked by also using the full solution to the corresponding differential equations describing mole balances in plug-flow reactors to estimate the rate constants in Scheme 1. This analysis gave the same values within experimental accuracy for all rate constants as those derived from extrapolation methods and eq 1.

Results and Discussion

Previous work^{9,10} has suggested that the rate of C–H activation for a given alkane is governed by the rate of activation of the weakest C–H bond. This implies that an Arrhenius plot of $(k_1 + k_2)/n_w$, where n_w is the number of weakest C–H bonds, would give a systematic trend between the apparent activation energy and the energy of the weakest C–H bond for various alkanes. Figure 1a shows an Arrhenius plot of $(k_1 + k_2)/n_w$ for various alkanes; Table 1 reports apparent activation energies and pre-exponential factors derived from Figure 1a. As can be seen from the inset in Figure 1a, a semilogarithmic plot of $(k_1 + k_2)/n_w$ at 648 K as a function of the energy of the weakest C–H bond shows the expected effects of the bond strength of the weakest C–H bond on alkane reactivity. However, while $(k_1 + k_2)/n_w$ decreased exponentially with the energy of the weakest C–H bond at a fixed reaction temperature, the apparent activation energy (see Table 1) did not vary systematically with the energy of the weakest C–H bond for a given alkane. We conclude, therefore, that the effects of C–H bond energies on activation energies for C–H bond activation cannot account for the observed differences in reactivity reflected in the measured values of $(k_1 + k_2)/n_w$ for the various alkanes.

These apparent inconsistencies can be resolved by considering the combined reactivity of all C–H bonds in a given alkane and the effects of temperature on their respective contributions to overall rates. First, we relate all apparent rate constants in eq 1 to those for the elementary steps in Scheme 2. Alkane reactions involve their initial quasi-equilibrated physisorption followed by the kinetically relevant C–H activation step that forms alkoxide intermediates.^{3,6} Subsequent reactions of alkoxides can form an alkene via H abstraction reactions (1') or CO_x reactions (2') via a sequence of irreversible steps involving

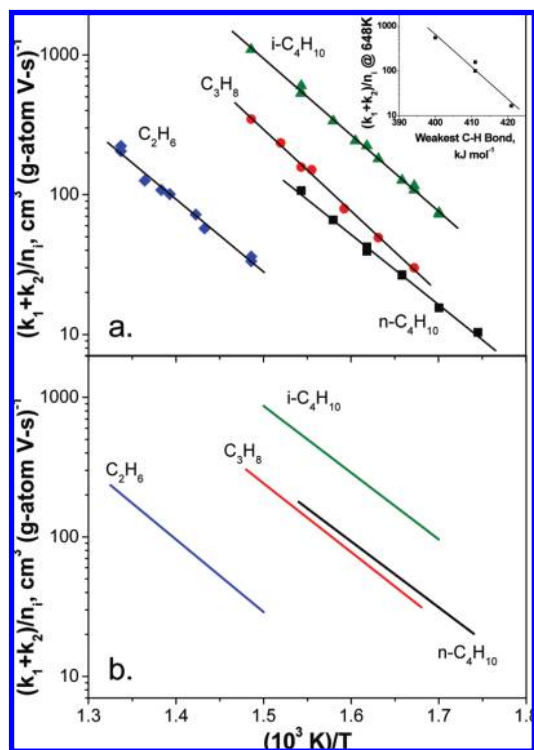


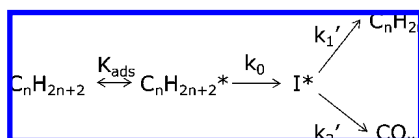
Figure 1. (a) Alkane reaction rate constant ($k_1 + k_2$) divided by the number of weakest C–H bonds (n_w) in C_2H_6 , C_3H_8 , $n-C_4H_{10}$, and $i-C_4H_{10}$, 6, 2, 4, and 1, respectively. (Inset) Normalized C–H bond activation rate constant at 648 K as a function of the weakest C–H bond strength in the alkane. (b) Estimate of $(k_1 + k_2)/n_w$ as a function of inverse temperature from eq 7.

TABLE 1: Apparent Activation Energies and Pre-Exponential Factors for the Normalized Alkane Consumption Rate Constants, $(k_1 + k_2)/n_w$ ^a

alkane	E_{app} , kJ mol ⁻¹	A_{app} , cm ³ (mol V-s) ⁻¹	weakest C–H bond strength, kJ mol ⁻¹
C_2H_6	99 ± 9	1.8×10^9 (4.4×10^8 , 7.2×10^9)	421
C_3H_8	112 ± 6	3.2×10^{11} (1.1×10^{11} , 9.7×10^{11})	411
$n-C_4H_{10}$	96 ± 5	2.2×10^{10} (8.0×10^9 , 5.9×10^{10})	411
$i-C_4H_{10}$	104 ± 3	1.5×10^{11} (5.3×10^{10} , 3.9×10^{11})	400

^a Confidence intervals are included at the 95% level.

SCHEME 2: Alkane Activation Pathways in ODH with Additional Mechanistic Details^a



^a Apparent rate constants k_1 and k_2 are broken into elementary steps including alkane physisorption (K_{ads}) and C–H bond activation (k_0).

sequential H abstraction and oxygen insertion. Measured k_1 and k_2 rate constants are related to the steps in Scheme 2 by

$$k_1 = K_{ads}k_0 \frac{k_1'}{k_1' + k_2'} \quad (2)$$

$$k_1 + k_2 = K_{ads}k_0 \quad (3)$$

In eq 3, K_{ads} is the alkane physisorption constant, k_0 is the rate constant for C–H activation in physisorbed alkanes, and

TABLE 2: Heats of Adsorption and Pre-Exponential Factors for Alkane Adsorption^a

alkane	ΔH_{ads} , kJ mol ⁻¹	K_{ads} , m	K_{ads} at 648 K, m
C_2H_6	-14.7	0.25	3.8
C_3H_8	-18.8	0.22	7.1
$n-C_4H_{10}$	-22.4	0.19	12
$i-C_4H_{10}$	-21.4	0.19	10

^a Heats of adsorption are based on the heat of alkane liquefaction taken from ref 22. Pre-exponential factors are calculated using partition functions.

k_1' and k_2' are the rate constants for alkoxide reactions to form alkenes and CO_x precursors, respectively. K_{ads} depends on the adsorption enthalpy, ΔH_{ads} , and adsorption entropy, ΔS_{ads} :

$$K_{ads} = e^{\Delta S_{ads}/R} e^{-\Delta H_{ads}/RT} \quad (4)$$

All alkanes investigated, except C_2H_6 , have more than one type of C–H bond (e.g., primary, secondary, and tertiary). Overall rate constants for C–H bond activation therefore contain contributions from each type of C–H bond in a manner that reflects their respective reactivities, activation barriers (E_i), pre-exponential factors (A_i), and number of equivalent bonds C–H bonds (n_i). The value of k_0 then becomes

$$k_0 = \sum_i n_i A_i e^{-E_i/RT} \quad (5)$$

Each E_i in eq 5 can be related to the bond dissociation energy of the i th type of C–H bond (D_i) using a Brønsted–Evans–Polanyi relation,^{12,13} which relates barriers for primary C–H bonds (E_1) to those for other types by

$$E_i = E_1 + \alpha(D_i - D_1) \quad (6)$$

In eq 6, E_2 and E_3 refer to barriers for secondary and tertiary C–H bonds, respectively, and α is a constant for homologous series of reactants.

Equations 5 and 6, together with the assumption that pre-exponential factors are independent of bond type ($A_i = A_1$, for all i), lead to an equation for k_0 in terms of the reactive properties of primary C–H bonds and the differences in energy among the various available C–H bonds

$$\frac{k_0}{n_w} = \frac{A_1}{n_w} e^{-E_1/RT} \sum_i n_i e^{-\alpha(D_i - D_1)/RT} \quad (7)$$

Equations 3, 4, and 7 can be used to describe the effects of temperature on $(k_1 + k_2)/n_w$ for different alkanes. K_{ads} in eq 4 was estimated by using condensation enthalpies to represent ΔH_{ads} for each alkane (Table 2; ref 22), and ΔS_{ads} was determined from the partition functions for alkanes in physisorbed and gaseous states, assuming that physisorbed species retain two degrees of translation and three degrees of rotation. The values of E_1 and A_1 in eq 7 were obtained from rate data for C_2H_6 reactants, which contain only primary C–H bonds. A_1 was estimated by dividing the apparent pre-exponential factor (1.8×10^9 cm³ (g-atom V-s)⁻¹; Table 1) by the estimate for $e^{\Delta S_{ads}/R}$, which led to a value of 2.0×10^7 cm² (g-atom V-s)⁻¹ for A_1 . E_1 was estimated by subtracting alkane adsorption

TABLE 3: Apparent Activation Energy and Pre-Exponential Factors Determined from the Estimated Values of $(k_1 + k_2)/n_w$ Presented in Figure 1b

alkane	E_{app} , kJ mol ⁻¹	A_{app} , cm ³ (mol V-s) ⁻¹
C ₂ H ₆	99	1.8×10^9
C ₃ H ₈	94	5.9×10^9
<i>n</i> -C ₄ H ₁₀	90	3.2×10^9
<i>i</i> -C ₄ H ₁₀	92	1.3×10^{10}

enthalpies from measured activation energies (99 kJ mol⁻¹; Table 1) to give an intrinsic barrier of 114 kJ mol⁻¹ for E_1 . The value of α in eq 7 was assumed to be 0.24, the value of α for H-atom transfer reactions²³ and a typical α value for BEP relations.²⁴

The Arrhenius plots for $(k_1 + k_2)/n_w$ obtained from eqs 3, 4, and 7 and the assumptions described above (leading to the parameters in Table 2) are shown in Figure 1b. The Arrhenius plot for C₂H₆ is the same as in Figure 1a, because experimental A_1 and E_1 values are used for this molecule. Equation 7 is fundamentally non-Arrhenius for C₃H₈, *n*-C₄H₁₀, and *i*-C₄H₁₀, but this behavior cannot be detected in an experimentally accessible temperature range. The predicted values of $(k_1 + k_2)/n_w$ for C₃H₈, *n*-C₄H₁₀, and *i*-C₄H₁₀, without additional assumptions, agree qualitatively with those determined from the experimental data (see Figure 1); however, the ordering of C₃H₈ and *n*-C₄H₁₀ is inverted, and the predicted apparent activation energies are somewhat lower than those determined from experimental data. Table 3 shows that estimated activation energies decrease with alkane size and are lower for *n*-C₄H₁₀ than *i*-C₄H₁₀, while estimated pre-exponential factors increase in the order C₂H₆ < *n*-C₄H₁₀ < C₃H₈ < *i*-C₄H₁₀.

The observed differences between the model and the experimental results are likely due to errors in the estimated heats of physisorption. An error of 3 kJ mol⁻¹ could cause an underestimate of the activation energy for the alkane size increases observed in Table 3 as well as the inversion of the ordering of C₃H₈ and *n*-C₄H₁₀ in Figure 1b.

While it may be attractive to attribute the 30-fold difference in reactivity of the alkanes to the 20 kJ mol⁻¹ difference in weakest C–H bond energies (see inset, Figure 1a), this conclusion is not supported by the measured apparent activation energies of the alkanes. There are no clear differences in measured activation energies that can account for the 30-fold increase in rates at 648 K. The interpretation presented above demonstrates that the trends in the measured data likely reflect differences in adsorption enthalpies and the number of C–H bonds in the alkanes and not simply the differences in bond energies for the weakest bonds.

Measured ratios of the rate constant for alkane combustion to alkane dehydrogenation (k_2/k_1) are shown as functions of temperature in Figure 2a. This ratio is only weakly dependent on temperature for all alkanes, indicating that activation energies for k_1 and k_2 are similar and suggesting that the transition states for the formation of alkenes reactions (1'; Scheme 2) and CO_x precursors reactions (2'; Scheme 2) are nearly identical in energy.

Previous studies suggest that alkene formation and initiation of CO_x formation involve a common intermediate, an alkoxide.^{3,4,6} We propose that the transition states for alkene formation and the first step toward CO_x formation involve H abstraction from the intermediate I* shown in Scheme 2 and that all H atoms are candidates for abstraction from this intermediate.

We assume that k_2/k_1 ratios result from the product of two factors, one sensitive to alkane identity and one not. The former factor accounts for the nature, number, and relative strength of

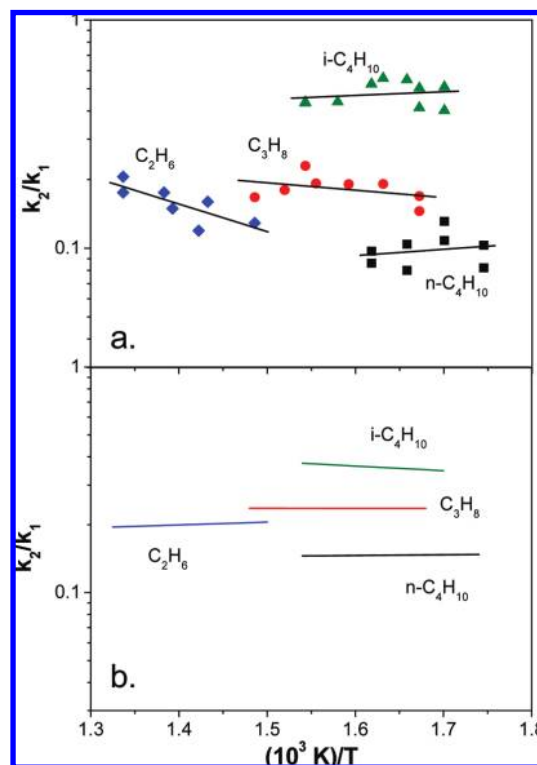


Figure 2. (a) Ratio of the rate coefficients for alkane combustion to alkane dehydrogenation, k_2/k_1 , as a function of inverse temperature. (b) Estimated values of k_2/k_1 as a function of inverse temperature calculated using eq 8 and the parameter values listed in Table 4.

TABLE 4: Fraction of Each Type of Alkoxide, f_i , and Number of C–H Bonds Forming Combustion Precursors ($n_{ij,C}$) and Alkene ($n_{ij,A}$) Products from Alkoxide i with C–H Bond Strength j^a

alkane	alkoxide type	alkoxide fraction, f_i	C–H bond strength, kJ mol ⁻¹	combustion precursors ($n_{ij,C}$)	alkenes ($n_{ij,A}$)	
C ₂ H ₆	primary	1	421		3	
			411	2		
C ₃ H ₈	primary	0.65	421	3		
			411	2	2	
	secondary	0.35	421		6	
			400	1		
<i>n</i> -C ₄ H ₁₀	primary	0.48	421	1.5	1.5	
			411	3	3	
	secondary	0.52	421	1.5	4.5	
			411		2	
			400	1		
<i>i</i> -C ₄ H ₁₀	primary	0.77	421	6		
			411	2		
				400		1
	tertiary	0.23	421		9	

^a The fraction, f_i , is an average value over the experimental temperature range. C–H bond strengths are derived from alkane C–H bond strengths with identical substitution at the carbon center.

C–H bonds available to form combustion precursors or alkenes, and the latter factor accounts for entropic differences in the transition states for the formation of alkenes and combustion precursors. The activation energies of C–H bonds in alkoxides will vary with bond strength and are estimated using BEP relations with the same parameters as those used for alkane C–H bond activation. C–H bond energies in surface alkoxides are assumed to be equal to those in the corresponding alkanes, and

H atoms at the α position relative to the C–O surface bond are assumed to have lower C–H bond energies, equal to the energy of a C–H bond with the next higher carbon substitution, e.g., a surface ethoxide has the equivalent of 3 primary C–H bonds (421 kJ mol⁻¹) and 2 secondary C–H bonds (411 kJ mol⁻¹). It is assumed that the activation entropy for formation of alkene and CO_x precursor is independent of the structure of the alkoxide from which these products originate; however, the activation entropy for alkene formation is considered to be larger than that for CO_x precursor formation because the entropy gained upon formation of a loosely bound molecule, leading to an alkene, is larger than that for a tightly bound surface intermediate, resulting in a precursor to CO_x. On this basis, the ratio k_2/k_1 is given by

$$\frac{k_2}{k_1} = \left(\frac{\sum_i f_i \sum_j n_{ij,C} e^{-E_{ij}/RT}}{\sum_i f_i \sum_j n_{ij,A} e^{-E_{ij}/RT}} \right) (e^{\Delta\Delta S^\ddagger/R}) \quad (8)$$

where f_i is the fraction of molecules that react via alkoxide type i ; $n_{ij,A}$ and $n_{ij,C}$ are the number of C–H bonds of type j yielding alkenes and combustion precursors, respectively, from the i th alkoxide type; E_{ij} is the activation energy for activation of the j th type of C–H bond in the i th alkoxide; and $\Delta\Delta S^\ddagger$ is the difference in the activation entropies for combustion precursor and alkene formation. From an analysis of the data presented in Figure 2, we estimate that $\exp(\Delta\Delta S^\ddagger/R)$ is ~ 0.2 , corresponding to $\Delta\Delta S^\ddagger = -13$ J (mol K)⁻¹, consistent with the expectation that the activation entropy for alkene formation is higher than that for combustion.

When more than one type of C–H bond is present in the reacting alkane, several surface alkoxide intermediates can be formed. With the exception of C₂H₆, each alkane forms two types of alkoxide: a primary alkoxide and a secondary or tertiary alkoxide. C₂H₆ forms only primary alkoxydes. The fraction of each intermediate, f_i , depends on the ratio of the C–H bond activation rate constants for each type of bond involved in their formation, $(k_1 + k_2)/(k_1 + k_2)_{\text{total}}$ (column 3; Table 4). The values of $n_{ij,A}$ and $n_{ij,C}$ are calculated for each alkane from the following assumptions about C–H activation in the alkoxide intermediates. After an alkoxide has been formed, in subsequent elementary steps H atoms will be abstracted from the alkoxide to produce an alkene or CO_x precursor. To estimate these H abstraction rates and their effect on product selectivity, we assume H abstraction rates are dependent on the C–H bond energy and that the position of the H atom abstracted determines the selectivity between combustion and alkene products. We propose that H abstraction at the β carbon in alkoxydes forms alkenes and at the α or γ carbons forms precursors to CO_x. For butoxydes formed from n -C₄H₁₀, H abstraction may lead to an alkoxide bound at two nonadjacent carbon atoms. Butoxydes bound in two positions may undergo intramolecular H-atom transfer to release alkenes or abstraction of additional H atoms to form butadiene or CO_x precursors. We assume that internal H-atom transfers have comparable activation barriers to H abstraction and therefore conclude that one-half of the γ - and δ -H abstraction events lead to alkenes and one-half to CO_x precursors. The values of $n_{ij,A}$ and $n_{ij,C}$ are summarized in Table, where nonintegral values of $n_{ij,A}$ and $n_{ij,C}$ for n -butane-derived alkoxydes are averages.

The values of k_2/k_1 estimated using eq 8 are shown in Figure 2b. These estimates are almost independent of temperature even though temperature appears explicitly in eq 8 and also affects

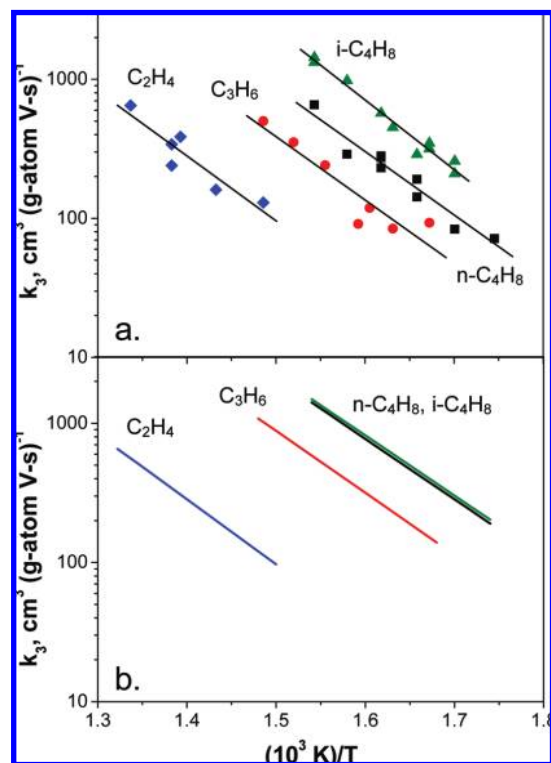


Figure 3. (a) Rate coefficient for alkene combustion, k_3 , as a function of inverse temperature. (b) Estimated values for k_3 as a function of inverse temperature.

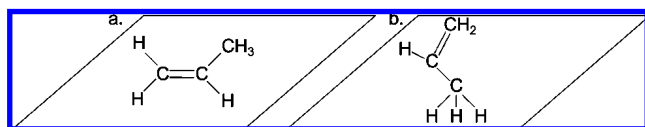
the values of f_i appearing in this expression. The ratio of k_2/k_1 predicted by eq 8 captures semiquantitatively the trends in measured values with alkane composition shown in Figure 2a. Differences in the sign of the slopes of the lines appearing in Figure 2b versus those appearing in Figure 2a are most likely due to the values of E_{ij} used in eq 8. These findings indicate that alkane C–H bond energies do not have a strong effect on k_2/k_1 but do influence this ratio by determining which alkoxydes are formed upon initial activation of an alkane molecule. Therefore, the primary selectivity of an alkane is determined by the fraction of alkane molecules passing through each alkoxide intermediate, and the selectivity of each alkoxide to products is determined by the number of C–H bonds activated to form a given product.

Figure 3a shows Arrhenius plots for alkene combustion rate constants (k_3) for the alkenes formed from the respective alkanes examined in this study. Apparent activation energies are similar for all alkenes (90 ± 25 kJ mol⁻¹), but combustion rate constants decrease in the sequence i -C₄H₈ > n -C₄H₈ > C₃H₆ >> C₂H₄, with k_3 being 23 times larger for i -C₄H₈ than C₂H₄ at 648 K.

We consider next how k_3 depends on the rate of C–H bond activation in alkenes. All C–H bonds in the alkene are assumed to be active, and activation energies are estimated on the basis of C–H bond energies (see eq 6). Alkenes have vinylic and allylic C–H bonds which are not found in alkanes. The bond energies for all vinylic C–H bonds are assumed to be 464 kJ mol⁻¹ (C₂H₄, ref 11) regardless of substitution at the carbon center. The bond energy for all allylic C–H bonds is 369 kJ mol⁻¹ (C₃H₆, ref 11), and we will use 2-C₄H₈ as the model for all normal butenes because it is $\sim 65\%$ of all butene products; however, this will lead to an underestimate of k_3 for n -C₄H₁₀ of $\sim 10\%$.

Alkene C–H bond strengths vary to a significantly greater degree than alkane C–H bond strengths (95 kJ mol⁻¹ versus 20 kJ mol⁻¹ in i -C₄H₁₀), and therefore, it may be expected that

SCHEME 3: (a) Hypothesized Precursor State for Vinylic C–H Bond Activation, and (b) Hypothesized Precursor State for Allylic C–H Bond Activation



only the weakest C–H bonds will contribute to the reactivity of alkenes. The ratio of k_3 for i -C₄H₈ to C₂H₄ estimated solely using BEP relations for activation energies is ~ 100 at 648 K, which is significantly larger than the actual ratio of 23 at 648 K. Activation energies for C₃H₆, i -C₄H₈, and n -C₄H₈ would also be expected to be lower than that for C₂H₄ by 20 kJ mol⁻¹. Since these expectations differ significantly from the observed rate constants we consider an alternative approach.

For alkenes other than C₂H₄, we assume that there are two physisorbed precursors for C–H bond activation. One is a weakly bound state for allylic C–H bond activation which interacts via H-bonding and van der Waals interactions. The second is a precursor for vinylic C–H bond activation which interacts with Lewis acid centers via π bonds of the alkene. The former will represent a relatively weak binding and hence has a smaller adsorption constant, $K_{\text{ads,all}}$, compared to the latter, $K_{\text{ads,vin}}$, because the van der Waals interactions are inherently weaker than Lewis acid–base interactions of π bonds in the alkenes. Possible structures for these precursor states are shown in Scheme 3. The rate constant k_3 is the sum over reaction rate over all adsorbed states i and C–H bond types, j , in the alkene

$$k_3 = \sum_i K_{\text{ads},i} \sum_j n_{ij} A_{ij} e^{-E_{ij}/RT} \quad (9)$$

where $K_{\text{ads},i}$ is the adsorption constant for the i th precursor state and n_{ij} , A_{ij} , and E_{ij} retain their previous definitions for C–H bond activation in alkanes. The subscript notation has been expanded to identify the precursor state, i , and the C–H bond activated in the i th precursor state, j .

Activation energies, E_{ij} , for H abstraction from alkenes were estimated using eq 6. The pre-exponential factor for allylic C–H bond activation was estimated as 2.0×10^7 cm² (mol V-s)⁻¹ under the assumption that the interactions of these species are similar to those for alkanes. The pre-exponential factor for vinylic C–H bond activation was determined to be 3.0×10^8 cm³ (g-atom V-s)⁻¹ from the apparent pre-exponential factor for C₂H₄ because it has only vinylic C–H bonds.

Heats of adsorption for allylic C–H bond activation precursors were estimated using the enthalpy change occurring upon condensation of the alkene (for C₃H₆, i -C₄H₈, and n -C₄H₈ they are 18.5, 22.4, and 23 kJ mol⁻¹, respectively; ref 22). The adsorption enthalpy for all species adsorbed as precursors to vinylic C–H bond activation was estimated from the difference between the activation energy of H abstraction from C₂H₄ from eq 6 (117 kJ mol⁻¹) and its apparent activation energy for combustion (89 kJ mol⁻¹), -28 kJ mol⁻¹. For reference, the difference between enthalpies of adsorption of C₂H₄ and C₂H₆ ranges from -52 kJ mol⁻¹ on monolayer V₂O₅(001)/TiO₂(001) anatase to -14 kJ mol⁻¹ on bulk V₂O₅(001).²⁵ Therefore, our estimate that the adsorption enthalpy of C₂H₄ is 13 kJ mol⁻¹ lower than that of C₂H₆ (-15 kJ mol⁻¹) is not unreasonable given available information.

Estimates of k_3 based on eq 9 are shown in Figure 3b. The predicted values of k_3 for C₂H₄ and i -C₄H₈ agree well with the

measured values shown in Figure 3a, but the estimated values of k_3 for C₃H₆ and n -C₄H₈ are ~ 1.5 times larger than those measured. This is likely due to underestimation of the adsorption enthalpies for precursors to vinylic C–H activation for larger molecules, which in this temperature range corresponds to a difference of less than 5 kJ mol⁻¹.

The estimates of k_3 show that an important factor in limiting the selectivity of ODH is the strong binding of alkenes. The presence of allylic C–H bonds does not increase the reactivity of alkenes significantly because activation energies for k_3 are ~ 90 kJ mol⁻¹ for all alkenes, regardless of the number of allylic C–H bonds. Precursors for allylic C–H bond activation are weakly bound, and the net effect is that the apparent activation energies for both vinylic and allylic C–H bonds are nearly identical.

Conclusions

Observed differences in the rates of C₂H₆, C₃H₈, n -C₄H₁₀, and i -C₄H₁₀ oxidative dehydrogenation occurring on VO_x/Al₂O₃ can be interpreted using a limited set of assumptions in combination with reasonable estimates of the kinetic parameters appearing in Scheme 2. The initial step in the reaction sequence, the activation of a C–H bond, depends on the strength of the C–H bond, and all C–H bonds within the molecule are candidates for activation. Thus, the apparent activation energy is a rate-weighted average over all C–H bonds in the molecule. Alkenes and CO_x are assumed to be produced by a series of irreversible reactions that start from alkoxide species formed upon activation of a C–H bond in the reactant alkane. The ratio of the rate coefficients for alkane combustion to alkene formation (k_2/k_1) is found to depend on the composition and structure of the alkane but is nearly independent of temperature. The ratio k_2/k_1 is directly influenced by the number and type of C–H bonds present in each alkoxide intermediate; however, k_2/k_1 is also indirectly affected by the strengths of the C–H bonds in the alkane because they determine the relative rates of formation of different alkoxide intermediates. The rate constant for alkene combustion (k_3) is influenced more strongly by the strength of alkene adsorption than by the strength of the C–H bonds in the alkene. While the presence of allylic C–H bonds in alkenes suggests high reactivity, the stronger binding of alkenes plays a more important role in determining the rate of alkene combustion. C₂H₄ has no allylic C–H bonds, and hence, its reactivity is expected to be negligible; however, it has significant reactivity relative to other alkenes because it has relatively strong binding via its π bonds, which explains the low yields observed for C₂H₄.

Acknowledgment. The authors thank Connie Lim for assistance with experiments. This work was supported by the Director, Office of Basic Energy Sciences, Chemical Sciences Division of the US Department of Energy under Contract DE-AC03-76SF00098.

Supporting Information Available: Description of the methods used to prepare and characterize the catalyst used in this study. This material is available free of charge via the Internet at <http://pubs.acs.org>.

References and Notes

- (1) Cavani, F.; Ballarini, N.; Cericola, A. *Catal. Today* **2007**, *127*, 113.
- (2) Blasco, T.; Nieto, J. M. L. *Appl. Catal. A: Gen.* **1997**, *157*, 117.
- (3) Chen, K. D.; Khodakov, A.; Yang, J.; Bell, A. T.; Iglesia, E. J. *Catal.* **1999**, *186*, 325.
- (4) Chen, K. D.; Bell, A. T.; Iglesia, E. J. *Phys. Chem. B* **2000**, *104*, 1292.

- (5) Chen, K. D.; Iglesia, E.; Bell, A. T. *J. Catal.* **2000**, *192*, 197.
- (6) Argyle, M. D.; Chen, K. D.; Bell, A. T.; Iglesia, E. *J. Phys. Chem. B* **2002**, *106*, 5421.
- (7) Chen, K. D.; Iglesia, E.; Bell, A. T. *J. Phys. Chem. B* **2001**, *105*, 646.
- (8) Chen, K.; Xie, S.; Bell, A. T.; Iglesia, E. *J. Catal.* **2001**, *198*, 232.
- (9) Batiot, C.; Hodnett, B. K. *Appl. Catal. A: Gen.* **1996**, *137*, 179.
- (10) Costine, A.; Hodnett, B. K. *Appl. Catal. A: Gen.* **2005**, *290*, 9.
- (11) Luo, Y.-R. *Comprehensive handbook of chemical bond energies*; CRC Press: Boca Raton, 2007.
- (12) Brønsted, J. N. *Chem. Rev.* **1928**, *5*, 231.
- (13) Evans, M. G.; Polanyi, M. *Trans. Faraday Soc.* **1938**, *34*, 0011.
- (14) Hammett, L. P. *J. Am. Chem. Soc.* **1937**, *59*, 96.
- (15) Barteau, M. A. *Catal. Lett.* **1991**, *8*, 175.
- (16) Nørskov, J. K.; Bligaard, T.; Logadottir, A.; Bahn, S.; Hansen, L. B.; Bollinger, M.; Benggaard, H.; Hammer, B.; Sljivancanin, Z.; Mavrikakis, M.; Xu, Y.; Dahl, S.; Jacobsen, C. J. H. *J. Catal.* **2002**, *209*, 275.
- (17) Pallassana, V.; Neurock, M. *J. Catal.* **2000**, *191*, 301.
- (18) Yang, S. W.; Iglesia, E.; Bell, A. T. *J. Phys. Chem. B* **2005**, *109*, 8987.
- (19) Yang, S. W.; Iglesia, E.; Bell, A. T. *J. Phys. Chem. B* **2006**, *110*, 2732.
- (20) Olthof, B.; Khodakov, A.; Bell, A. T.; Iglesia, E. *J. Phys. Chem. B* **2000**, *104*, 1516.
- (21) Khodakov, A.; Yang, J.; Su, S.; Iglesia, E.; Bell, A. T. *J. Catal.* **1998**, *177*, 343.
- (22) Yaws, C. L. *Chemical properties handbook physical, thermodynamic, environmental, transport, safety, and health related properties for organic and inorganic chemicals*; McGraw-Hill: New York, 1999.
- (23) Roberts, B. P.; Steel, A. J. *J. Chem. Soc., Perkin Trans. 2* **1994**, 2155.
- (24) Butler, E. T.; Polanyi, M. *Trans. Faraday Soc.* **1943**, *39*, 0019.
- (25) Sayle, D. C.; Catlow, C. R. A.; Perrin, M. A.; Nortier, P. *Catal. Lett.* **1996**, *38*, 203.

JP901595K